Energies **2009**, *2*, 714-737; doi:10.3390/en20300714

OPEN ACCESS

energies

ISSN 1996-1073

www.mdpi.com/journal/energies

Article

Enhanced Oil Recovery (EOR) by Miscible CO_2 and Water Flooding of Asphaltenic and Non-Asphaltenic Oils

Edwin A. Chukwudeme and Aly A. Hamouda *

Department of Petroleum Engineering, University of Stavanger, 4036 Stavanger, Norway;
E-Mail: edwin.a.chukwudeme@uis.no

* Author to whom correspondence should be addressed; E-Mail: aly.hamouda@uis.no;
Tel.: +47-5183-22 71; Fax: +47-5183-1750.

Received: 6 May 2009; in revised form: 4 August 2009 / Accepted: 27 August 2009 / Published: 2 September 2009

Abstract: An EOR study has been performed applying miscible CO_2 flooding and compared with that for water flooding. Three different oils are used, reference oil (*n*-decane), model oil (*n*-C10, SA, toluene and 0.35 wt % asphaltene) and crude oil (10 wt % asphaltene) obtained from the Middle East. Stearic acid (SA) is added representing a natural surfactant in oil. For the non-asphaltenic oil, miscible CO_2 flooding is shown to be more favourable than that by water. However, it is interesting to see that for first years after the start of the injection (< 3 years) it is shown that there is almost no difference between the recovered oils by water and CO_2, after which (> 3 years) oil recovery by gas injection showed a significant increase. This may be due to the enhanced performance at the increased reservoir pressure during the first period. Maximum oil recovery is shown by miscible CO_2 flooding of asphaltenic oil at combined temperatures and pressures of 50 °C/90 bar and 70 °C/120 bar (no significant difference between the two cases, about 1%) compared to 80 °C/140 bar. This may support the positive influence of the high combined temperatures and pressures for the miscible CO_2 flooding; however beyond a certain limit the oil recovery declined due to increased asphaltene deposition. Another interesting finding in this work is that for single phase oil, an almost linear relationship is observed between the pressure drop and the asphaltene deposition regardless of the flowing fluid pressure.

Keywords: EOR miscible CO_2; asphaltene; relative permeability; pressure drop; wettability; CO_2; EOR; mobility ratio; relative permeability

1. Introduction

CO_2 flooding has been field tested for oil recovery with varying degrees of success [1-2]. Application of CO_2 injection in heavy oil reservoirs has received less attention compared to light oil reservoirs. There are two reported reasons for this; it is believed that in heavy oil reservoirs, CO_2 lacks acceptable sweep efficiency due to the large viscosity contrast between CO_2 and oil as well as unlikely development of a miscible front in heavy oil reservoirs [3].

The extent of oil recovery is influenced by a number of parameters such as relative permeability, wetting conditions, viscous fingering, gravity tonguing, channelling and the amount of crossflow/mass transfer [4-6]. Tang *et al*. [7-8] observed that the morphology of flowing gas bubbles plays a dominant role on solution gas drive in heavy oils.

Relative permeability is one of the essential parameters required in numerical simulators to design and make a decision for any reservoir development. Singh *et al*. [5] compared the viscous and gravity dominated gas-oil relative permeabilities and suggested that gas flood relative permeability can be applicable to viscous dominated regions of the reservoir as long heterogeneities and flow rates are accounted for properly. Al-Wahaibi *et al*. [9] investigated the behaviour of two-phase drainage and imbibition relative permeabilities at near miscible conditions and concluded that as the interfacial tension decreases, the non wetting phase relative permeability increases more rapidly than the wetting phase relative permeability. Schembre *et al*. [10] examined the effects of temperature on heavy-oil relative permeability and found that diatomite rocks became more water-wet with temperature. Sola *et al*. [11] investigated temperature effects on the heavy oil/water relative permabilities of carbonate rocks and observed that the shape of oil relative permeability changes with increasing temperature. This was attributed to wettability alterations due to elevated temperature. Their results were in contrast to some previous studies dealing with sandstone systems where residual oil saturation was found to decrease and irreducible water saturation increases with temperature. Dana and Skoczylas [12] show that, for a viscosity ratio $\mu_{nw}/\mu_w << 1$, the gas relative-permeability remains unchanged even if the wetting fluid viscosity is twenty times higher than that of water.

Viscous fingering is a phenomenon that arises due to the instability of the interface between two fluids that have different viscosities. This takes place either on the front or rear of sample plug when there is a sufficiently high viscosity contrast between the displacing and displaced fluid [13-14]. Viscous fingering and dispersive by-passing is found to increase with oil viscosity [15]. The viscosity of the oil phase has a profound effect on coalescence dynamics of gas during bubble nucleation [16-17]. Brailovsky *et al*. [18-19], suggested that for both immiscible and miscible displacement, instability is caused by the high mobility of the displacing fluid. This is attributed mainly to viscosity and/or density stratification. Musuuza *et al*. [20] examined stability criteria for density driven flows in homogeneous porous media. It was suggested that a stable system is attained when there is a balance of external forces such as inertia, viscous stresses and buoyancy. The effect of asphaltene content on

the heavy oil viscosity has long been studied, which shows that increasing asphaltene contents result in an increase of oil viscosity [21-22]. Peng *et al*. [23] concluded from their studies on oil chemistry, that acid and base groups within asphaltene are a source of interfacial instability. Viscosity reduction in heavy oil by CO_2, has been reported to be much larger than in light oil [4,24-25].

Asphaltene precipitation has been a serious concern in the oil industry because it can undergo phase transitions that are an impediment in the production of crude oil [26]. De Boer *et al*. [27] observed that highly compressible, under-saturated crude oils are most susceptible to asphaltene deposition with pressure drop. The precipitation of asphaltenes begins at pressures between the reservoir pressure and the bubble point pressure of the reservoir oil. Typically, the amount of precipitated asphaltene increases as the pressure decreases [28]. Depending on the location of the pressure drops, asphaltene deposition may occur in different parts of the reservoir, as well as in the wellbore and the production stream [29-30]. It is explained based on the process that by decreasing the pressure the relative volume fraction of the light components within the crude oil increases. Danesh *et al*. [31] observed that asphaltene precipitation increased as the pressure drop increased in a Visual micro model. Newberry and Barker [32] also reported that the key causes of asphaltene precipitation are pressure decrease and the introduction of incompatible fluids. On the contrary, the asphaltene precipitation of two reservoir oil samples collected from Jilin oil field has been studied under pressure and with/without CO_2-injection conditions [33]. They observed that no asphaltene precipitation was detected during pressure depletion processes without CO_2 injection. For the CO_2 injected oil systems, appreciable asphaltene precipitation was detected when the operating pressure approached or exceeded the minimum miscible pressure (MMP). The amount of asphaltene precipitation increased with the concentration of injected CO_2.

In this study, the effect of oil composition, temperature and pressure on CO_2–oil relative permeability are investigated to address enhanced oil recovery by miscible CO_2 injection. Also, addressed is the effect of pressure drop on asphaltene precipitation.

2. Results and Discussion

This section is divided into two parts. The first part compares the oil recovery by miscible CO_2 flooding of non asphaltenic and asphaltenic oils at different pressures and temperatures. The outcrop chalk samples are modified by aging in asphaltenic and non-asphaltenic model oil to bench mark the effect of aging with asphaltene on oil recovery. This may resembles two field situations where the chalk is modified with the asphaltenic oil and the other situation is where the modification is occuring as the asphaltene deposits during CO_2 injection. The effect of different pressure drops on asphaltene precipitation with constant injection pressures and temperatures is addressed in this part. The second part deals with simulation of the experimental results using Eclipse compositional model (300).

2.1. Miscible CO_2 flooding of asphaltenic and non-asphaltenic oils

2.1.1. Effect of pressure (miscible/immiscible CO_2flooding) on oil recovery

Figure 1 shows a difference of 12% oil recovery between miscible and immiscible flooding with CO_2, where about 65% and 53% for miscible and immiscible flooding, at pressures of 90 and 26 bar,

are estimated respectively. In these experiments, the cores were saturated with (non-asphaltenic) 0.005 M SA dissolved in n-C_{10} (used as reference oil + natural surfactant) at room temperature of 25 °C. This demonstrates, as expected lower recovery, when flooding with CO_2 below minimum miscibility pressure (MMP). Hereafter, in the paper, the experimental works are done under miscible conditions.

Figure 1. Comparison between the oil recoveries of non-asphaltenic oil (0.005 M stearic acid (SA) dissolved in n-decane (n-C_{10})), for miscible and immiscible CO_2 flooding, at 25 °C, 90 and 26 bar respectively.

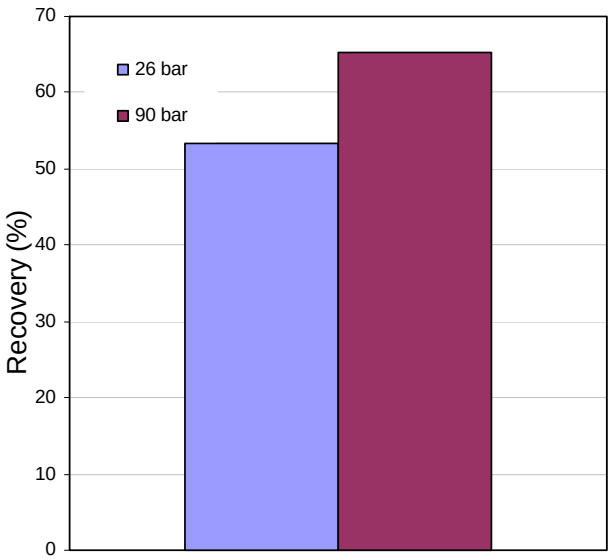

2.1.2. Effects of oil composition, pressure and temperature on oil recovery with CO_2 flooding

In this section the effect of three different combinations of temperatures and pressures for miscible flooding with CO_2 on oil recovery is illustrated for three different oils, reference oil (n-decane), model oil (0.005 M SA dissolved in n-C10, 0.35 wt % asphaltene dissolved in toluene) and crude oil (for its composition, see Table 3).

Figure 2(a-f) illustrate the oil recovery and the generated relative permeability curves (using Sendra Simulator version 1.10) from the different experimental conditions and for the different oils. Sendra Simulator inputs are the core properties, production data and pressure drop across the core as a function of time. The combinations of temperatures and pressures of 50 °C and 90 bar, 70 °C and 120 bar, or 80 °C and 140 bar are used to study the effect of different miscibility conditions on oil recovery.

Figure 2a shows same ultimate oil recovery of about 90% for the reference oil at both 70 °C/120 bar and 80 °C/140 bar flooding conditions compared with about 80% for the lower flooding conditions (50 °C/90 bar). No significant difference is observed in the relative permeability curves (Figure 2b) with the three combined temperatures and pressures. A cross point gas saturation of about 0.3 is shown. At CO_2 breakthrough, CO_2 seems to have displaced most oil from the largest accessible pores leaving low residual oil saturation.

In contrast, the model and crude oils saturated cores showed differences in the cross points for the relative permeability curves (Figure 2d,f) and CO_2 saturation as a function of the combined temperatures and pressures. The cross points for the relative permeability curves for model oil saturated cores are shown to decrease (move to the left) with increasing temperature and pressure. Residual oil saturation of 0.22, 0.21 and 0.33; cross point relative permeabilities of 0.019, 0.018 and 0.017 with corresponding CO_2 saturations of 0.28, 0.29 and 0.25 are estimated for combination of temperatures and pressures of 50 °C/90 bar, 70 °C/120 bar and 80 °C/140 bar, respectively. The observed higher residual oil saturation at 80 °C/140 bar may be due to asphaltene precipitation at these conditions. A similar trend is observed for crude oil saturated cores as to that for the model oil. Both oils has a common composition of asphaltene, however higher asphaltene content (10 wt %) in case of the crude oil compared with model oil (0.35 wt % asphaltene). As a result, different wettabilities occur; hence different relative permeability curves are obtained.

Figure 2e,f shows the CO_2–oil relative permeability corresponding to the oil recovery for the crude oil saturated cores. The cross point for the relative permeability curves are shown to be shifted more towards the left compared to the model oil. The residual oil saturation, CO_2 saturation and cross point relative permeability are observed at 0.62, 0.20 and 0.0019; 0.63, 0.19 and 0.0017 and 0.64, 0.18 and 0.00081, at 50 °C/90 bar, 70 °C/120 bar and 80 °C/140 bar, respectively. The general increase of both the shift in the relative permeability curves and the decrease in oil recovery compared with the other oils may support the explanation given above with respect to the effect of the asphaltene in both oil recovery and the relative permeability behaviour, especially at elevated temperatures and pressures. A summary of the above relative permeabilites and oil recovery shown in Figure 2, for clarity is presented in Figure 3, where oil recovery and relative permeability curves of CO_2 flooding of the different oils and at each individual combined temperature and pressure are compared. End points (kro and krg) are summarized in Table 1.

Table 1. Estimated end points relative permeabilities.

Oil	Temperature and Pressure	Kro end points	Krg end points
n-decane	50 °C, 90 bar	0.10	0.82
n-decane	70 °C, 120 bar	0.04	0.92
n-decane	80 °C, 140 bar	0.01	0.98
model	50 °C, 90 bar	0.10	0.86
model	70 °C, 120 bar	0.13	0.84
model	80 °C, 140 bar	0.13	0.84
crude	50 °C, 90 bar	0.25	0.20
crude	70 °C, 120 bar	0.25	0.19
crude	80 °C, 140 bar	0.23	0.17

Both Figure 3 and Table 1 illustrate the effect of asphaltene and its content on the oil recovery and the shift in both relative permeability end points and the cross points. Pooladi-Darvish and Firoozabadi [34] conducted similar experiments using a sandpack with light- and heavy-oil as well as simulation studies, varying gas-oil relative permeabilities and corey exponents to fit experimental

results. They found that gas mobility in heavy-oil was much less than in light oil. This is consistent with our observation and seems reasonable because heavy-oil with higher viscosity will tend to resist gas mobility. It may therefore be concluded, that the content of the asphaltene in the oil, pressure and temperature are major parameters affecting the oil recovery by CO_2 injection.

Figure 2. Effect of pressure and temperature on (a) oil recovery with *n*-decane, (b) CO_2–C_{10} relative permeability curves, (c) oil recovery for model oil, (d) CO_2–model oil relative permeability curves, (e) oil recovery for crude oil, (f) CO_2–crude oil relative permeability curves. The arrows indicate CO_2 cross point saturation.

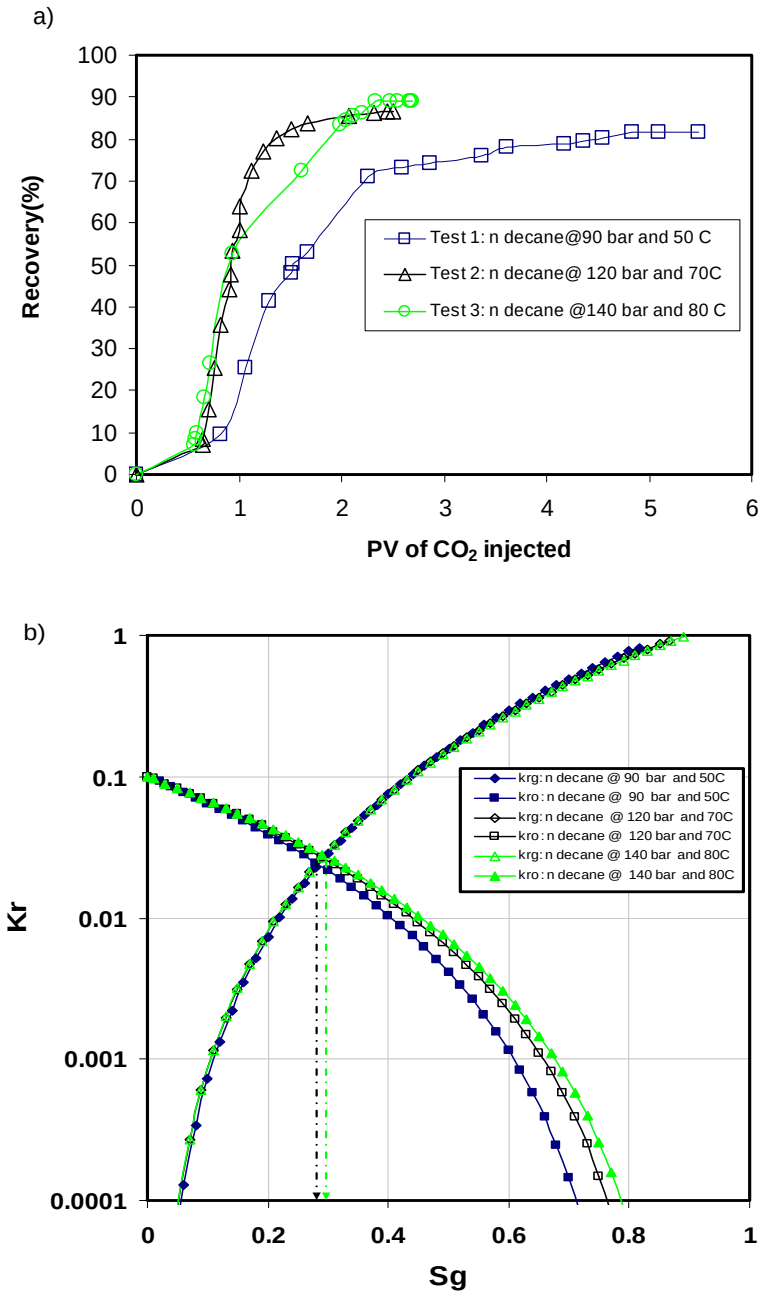

Figure 2. Cont.

c)

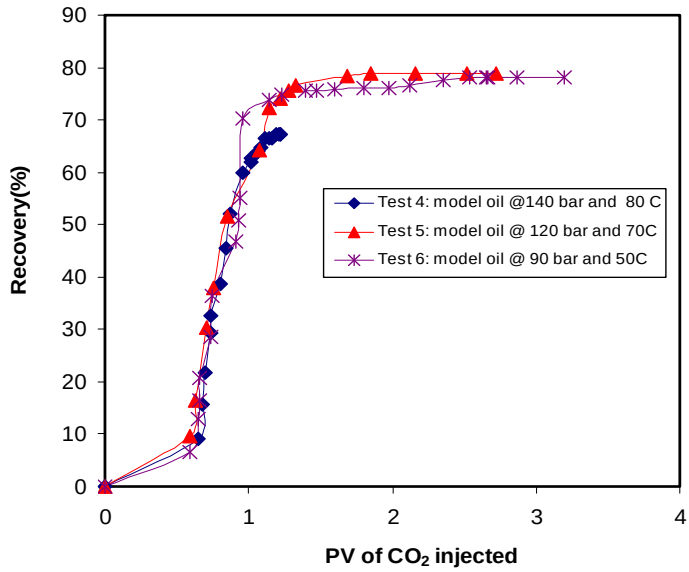

d)

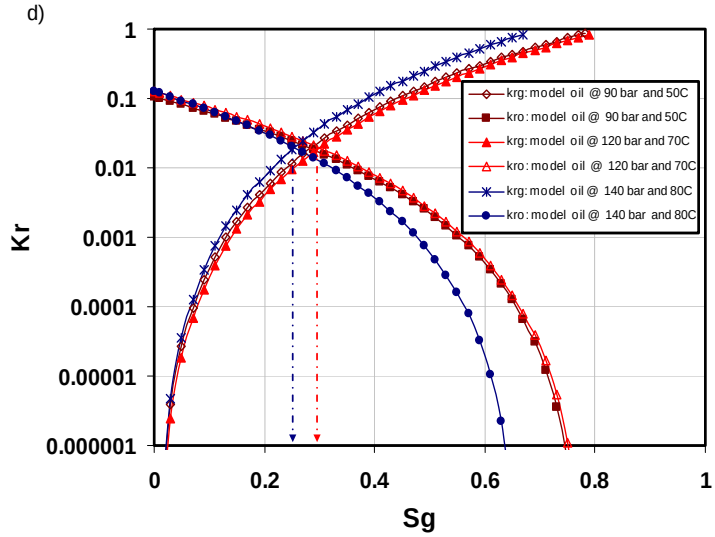

e)

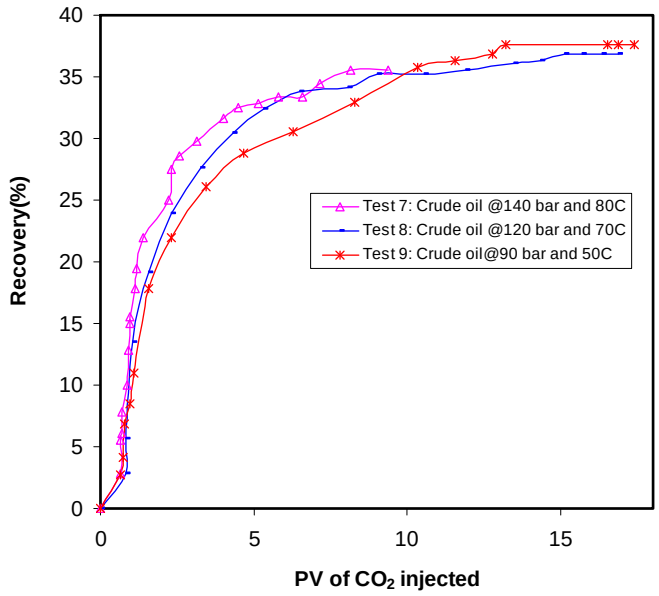

Figure 2. Cont.

f)

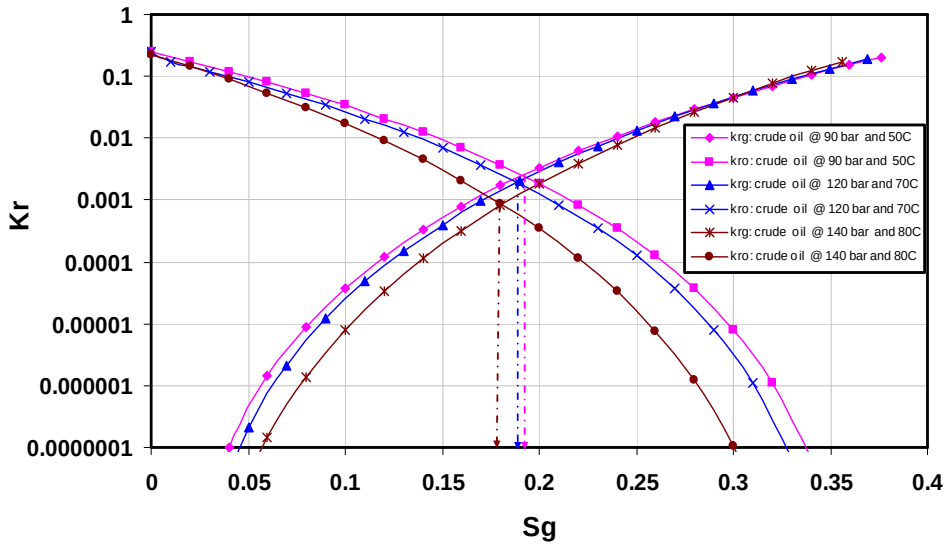

Figure 3. Summary of the effect of the different combination of temperatures and pressures on the relative permeability and oil recovery for the different oils: (a) oil recovery at 50 °C/90 bar, (b) CO_2–oil relative permeability curves at 50 °C/90 bar, (c) oil recovery at 70 °C/120 bar, (d) CO_2–oil relative permeability curves at 70 °C/120 bar, (e) oil recovery at 80 °C/140 bar, (f) CO_2–oil relative permeability curves at 80 °C/140 bar. Arrows point to Sg at the cross point.

a)

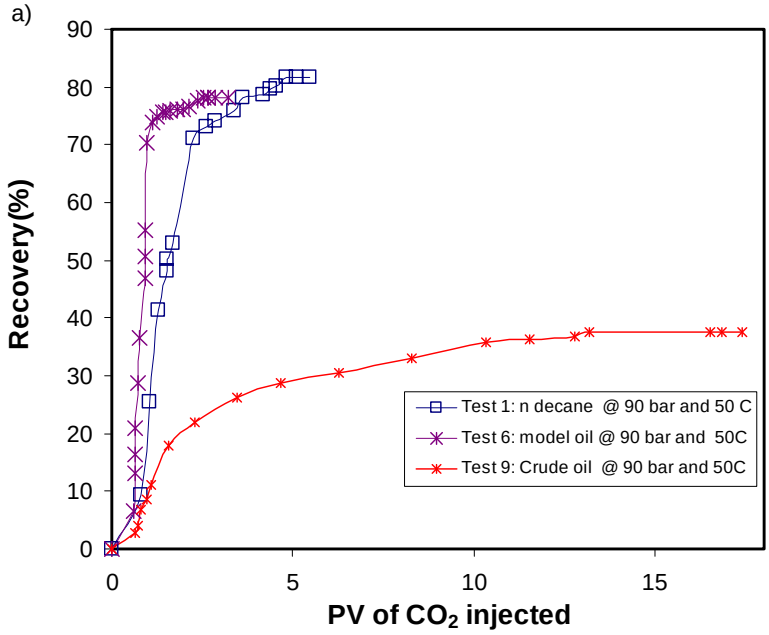

Figure 3. Cont.

b)

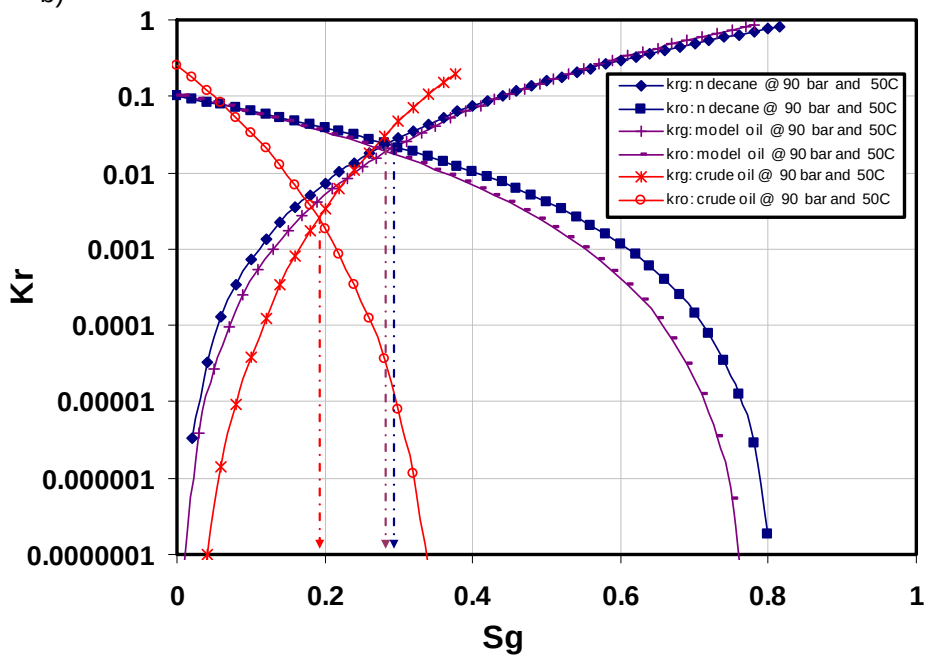

c)

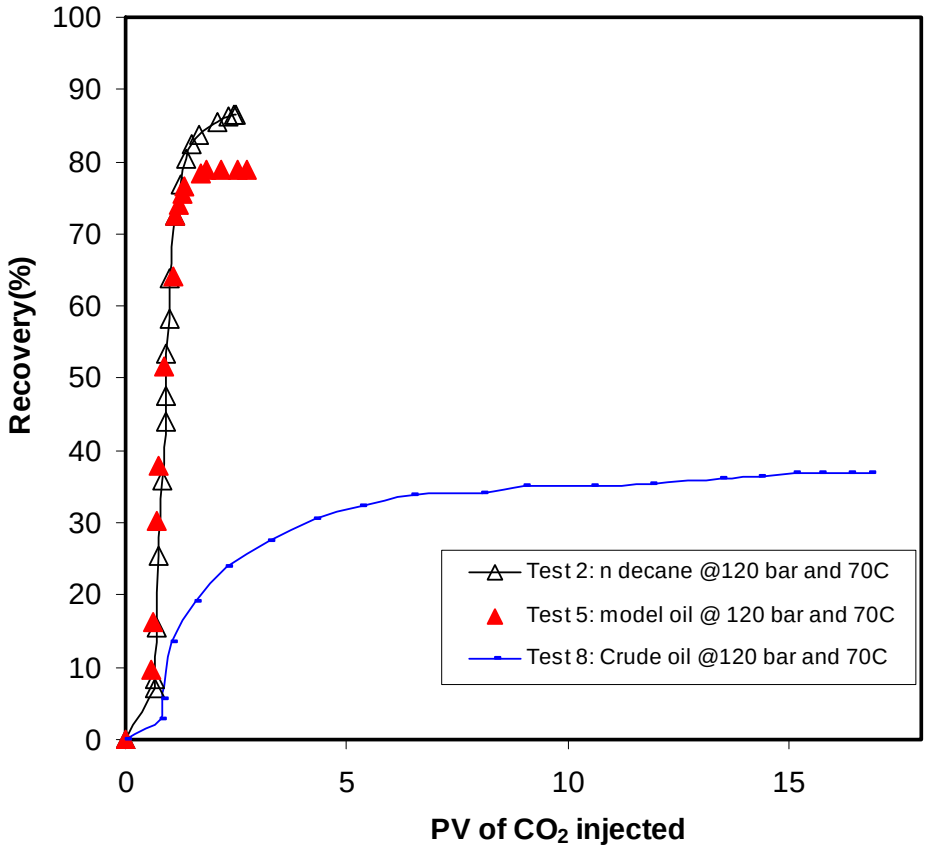

Figure 3. Cont.

d)

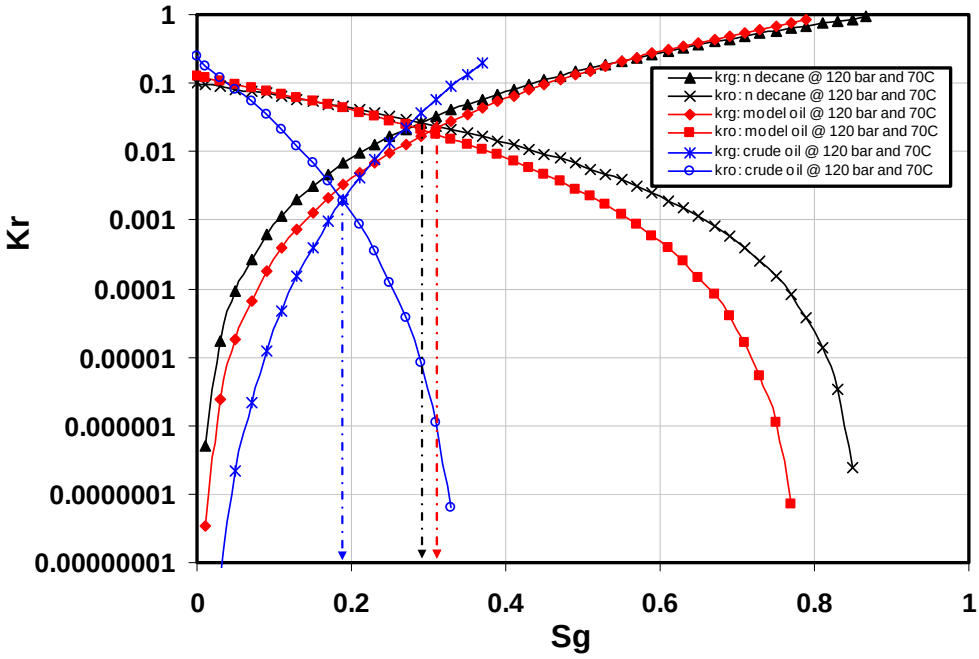

e)

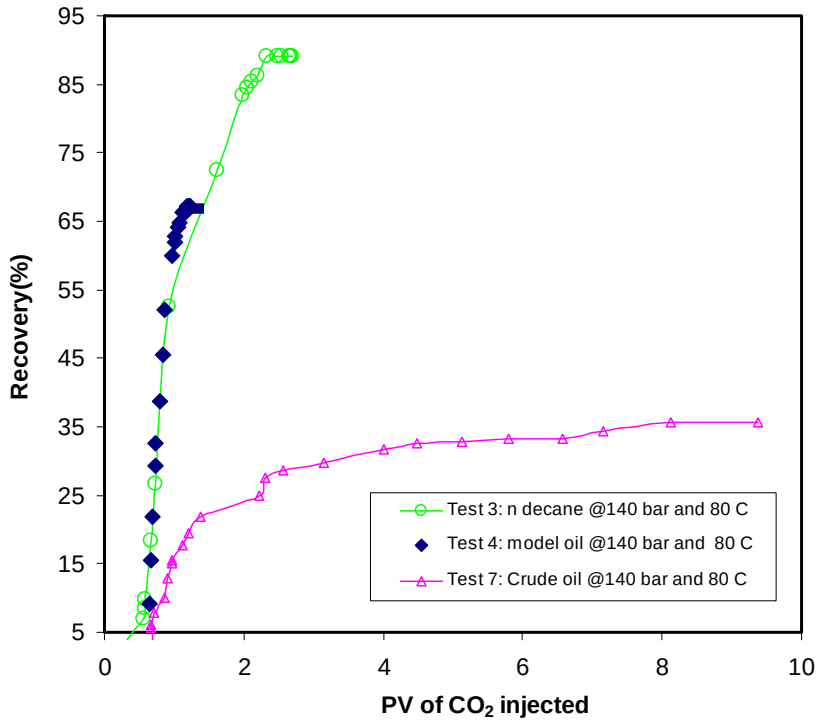

Figure 3. Cont.

f)

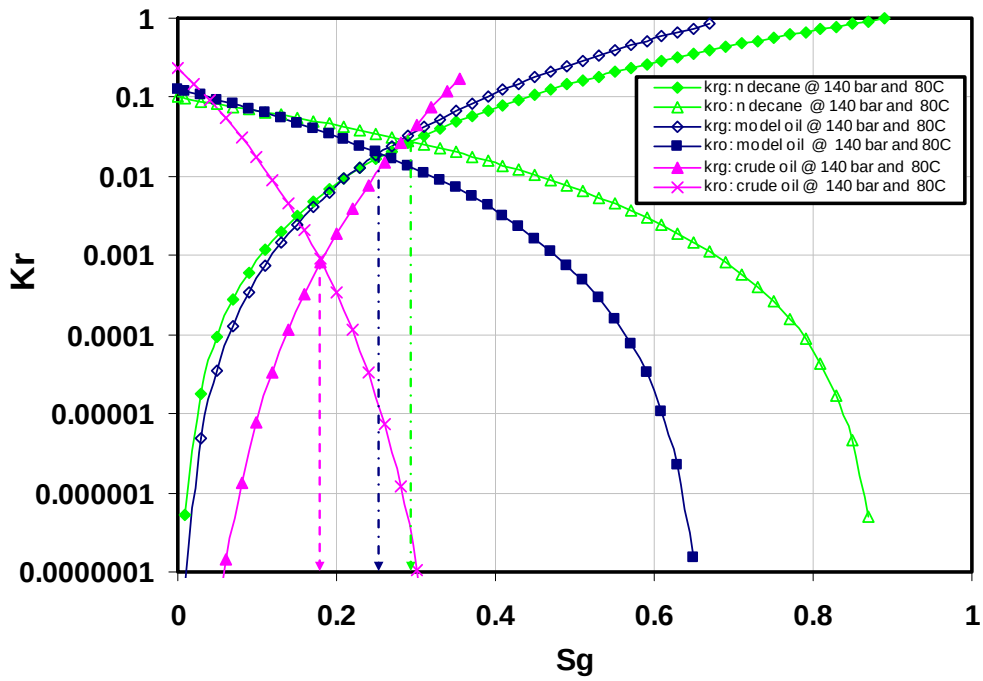

2.3. Comparison between oil recoveries for model oil flooded cores by water and CO_2

Experiments are done to compare the oil recovery by CO_2 and water for model oil. The results are shown in Figure 4. The water flooding experiments are performed using distilled water to exclude the complex effect of the ions.

A difference in oil recovery of about 1%, 4% and 7 %, are observed at temperatures of 50, 70 and 80 °C (90 °C) and corresponding pressure of 90, 120 and 140 bar, respectively, in the case of CO_2 flooding. There is inconsiderable difference between the two flooding processes at temperature ≤70 °C, with slightly higher oil recovered by CO_2 flooding. On the other hand at temperature >70 °C, oil recovered by CO_2 flooding is shown to be lower than that obtained by water flooding.

Water displacement at high temperature for asphaltenic oil reservoirs is shown, to give higher recovery. In this work CO_2 flooding is shown to be plausible for asphaltenic oil reservoir at lower temperature (<70 °C). Gielen and Unander [35] reported that oil recovery by miscible CO_2 flooding is limited to reservoirs with a temperature <120 °C, with no explanation given.

2.4. Asphaltene precipitation as a function of pressure drop for different flowing pressures

The pressure drop effect on the asphaltene deposition is investigated and shown in Figure 5. It is interesting to see that for the same asphaltene content in the oil and isothermal flowing condition (100 °C), it is the pressure drop that affects the asphaltene deposition and not the flowing pressures. More over, for the same pressure drop and different flowing pressure, almost the same amount of precipitated asphaltene (wt%) is estimated from the experiment.

The estimated precipitated asphaltene (wt%) shown as a function of pressure drop of 100 bar (with oil injection of 130 bar), 80 bar (with oil injection pressure of 130 bar), 80 bar (with oil injection

pressure of 100 bar), 50 bar (with oil injection pressure of 130 bar), 20 bar (with oil injection pressure of 120 bar) and 20 bar (with oil injection pressure of 100 bar) are 0.26, 0.19, 0.21, 0.18 ,0.14, and 0.14 wt%, respectively. A linear relation fit with $R^2 = 0.93$ is shown in Figure 5. The experimental error is approximately 10%. It must be mention that the experimental results are based on model oil (no dissolved light components). This perhaps resembles under-saturated fluids, where the pressure drop has negligible effect on the composition.

Figure 4. Comparison between oil recovery by water and CO_2 flooding for model oil saturated cores at 50, 70 and 80 °C (90 °C). The temperature of 90 °C in bracket is for water flooding experiments. The dotted line is an extension for the PV shift for CO_2 flooding at 140 bar and 80 °C.

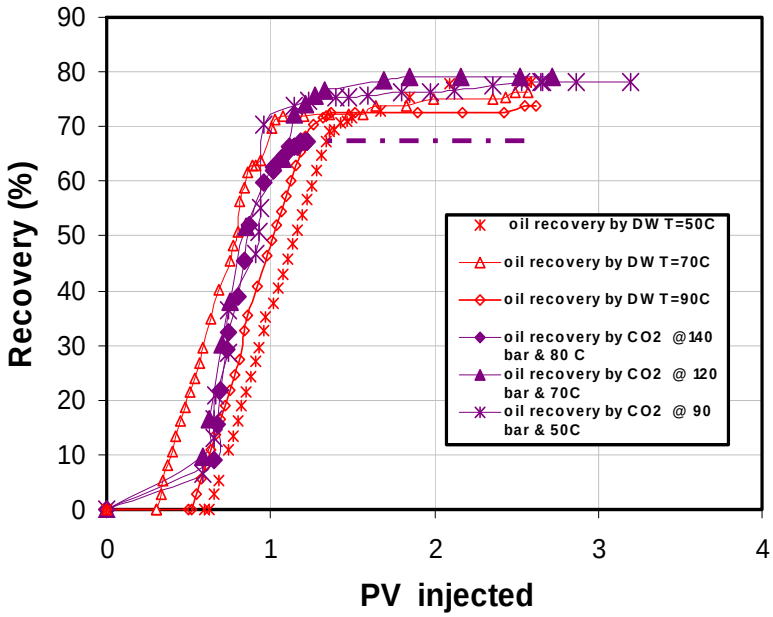

Figure 5. Asphaltene precipitation (wt %) at 100 °C with visual illustration on the influence of pressure drop on asphaltene precipitation. (a) Pressure drop of 20 bar; (b) Pressure drop of 100 bar; (c) Initial oil (model oil).

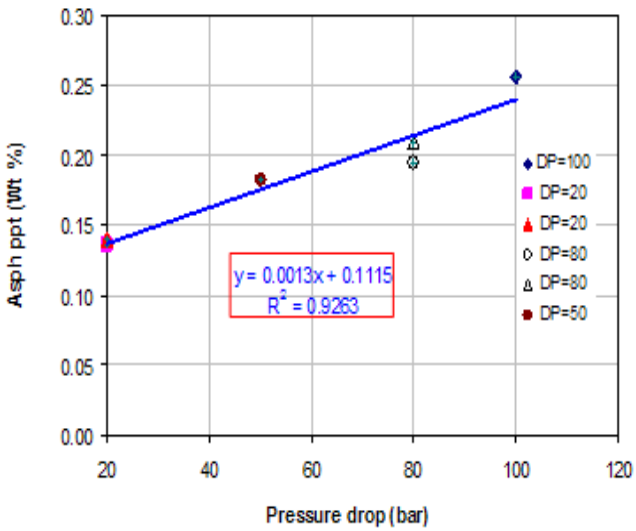

Visual illustration of the obtained oil colour is shown, in which at higher pressure drop, lighter colour oil is produced. This may indicate more asphaltene precipitation.

2.5. Simulation: effect of asphaltene precipitation by miscible CO_2 on oil recovery

Miscible CO_2 injection for recovery from reservoirs of non asphaltenic and asphaltenic oils are simulated in order to see the laboratory results in perspective of large scale. The simulated reservoir consists of total pore volume of 57.6 MM rb (total fluid) and hydrocarbon pore volume (HCPV) of approximately 46.1 MM rb with an average oil saturation of 0.8. Bottom hole pressure of 8,890 psia is specified as injection pressure constraint. Detailed simulation input data and procedures is stated in the experimental part (Section 3.4).

Figure 6a,b compare oil recovery by miscible CO_2 flooding with and without asphaltene using Eclipse asphaltene modeling option for 500 grid blocks. Cumulative recovered oil of about 10.5 MM STB is predicted for the non asphaltenic oil. Using the asphaltene modeling option of the simulator with three different CO_2 scenarios (1, 10 or 15 mol %) show cumulative recoverable oil of 45, 52 and 2M STB from the three scenarios, respectively. The simulation for both oil types were run for a period of
20 years. Speight [36] and Branco *et al*. [37] suggested precipitation of asphaltene as a function of carbon number of alkanes and reported that as the alkane carbon number increases, the precipitated amount of asphaltene decreases. Burke *et al*. [38] and Werner *et al*. [39] stated that CO_2 injection plays major role for asphaltene precipitation. Figure 6c shows the simulated ultimate oil recovery with corresponding field pressure response as function of mol% of CO_2. It is interesting to see that increasing CO_2 from 1 to 10 mol %, the ultimate recovered oil increased from >40,000 to >50,000 STB, which corresponds to increase of the field response pressure of about 10 folds, indicating asphaltene deposition. Above 10 mol % of injected CO_2 (simulated here at 15 mol %), a large drop in the ultimate oil recovery is predicted. This may suggest that from this simulation that the identified critical CO_2 concentration is within the lowest identified critical CO_2 from our previous work Hamouda *et al*. [40] as illustrated in Figure 6d. The critical CO_2 concentration is defined as a concentration above which asphaltene deposition starts that would affect the oil recovery. The simulation showed that after 600 days of CO_2 injection (15 mol % scenario), the injection pressure increased and reached the specified injection pressure constraint indicating asphaltene deposition. Previous work by Hamouda *et al*. [40], suggests that below a critical CO_2 content (identified average, highest and lowest critical point for CO_2 expressed as CO_2 mol %, were 33, 42 and 17, respectively) asphaltene is stable in the fluid. This demonstrates that miscible CO_2 flooding of asphaltenic oil is viable method for oil recovery below the critical CO_2 content, without major reservoir damage by asphaltene deposition. It also demonstrates that the recovery by miscible injection of CO_2 into non asphaltenic reservoir fluids is higher than that with asphaltenic oil (as shown in Figure 6), as expected.

2.6. Simulation: Comparison between oil recovery by water and miscible CO_2 flooding

Figure 7 shows the difference between oil recovery by water and miscible CO_2 flooding (well stream containing 100% CO_2) for same reservoir conditions with non-asphaltenic reservoir fluid.

Ultimate oil recoveries of approximately 10.5 and 6.4 MM STB are recovered for a period of 20 years by miscible CO_2 and water flooding, respectively. This is an increase in oil recovery of about 39%. It is interesting to see that extra oil recovery starts after about 3 years of injection. Lindeberg *et al*. [41] in their simulations observed that extra oil production starts after the seventh year. For non-asphaltenic oils, EOR by CO_2 initiated after at least three years of water injection, shows the benefit of miscible flooding, however consideration of economics, energy consumption and environment balance have to be brought into the equation for the decision on when to start injection if it is an option.

Figure 6. Simulated miscible CO_2 flooding on oil recovery for (a) non-asphaltenic oil, (b) miscible CO_2 injection with three different scenarios (1, 10 and 15 mol % of CO_2) for asphaltenic oil, (c) ultimate oil recovery with corresponding field pressure response as a function of mol % of CO_2 in the oil. The thick and dotted lines represent oil recovery (STB) and the corresponding injection pressure (psia), respectively. (d) Effects of pressure, temperature and mol % of CO_2 in the liquid on amount of asphaltene precipitation (wt %) [40].

a)

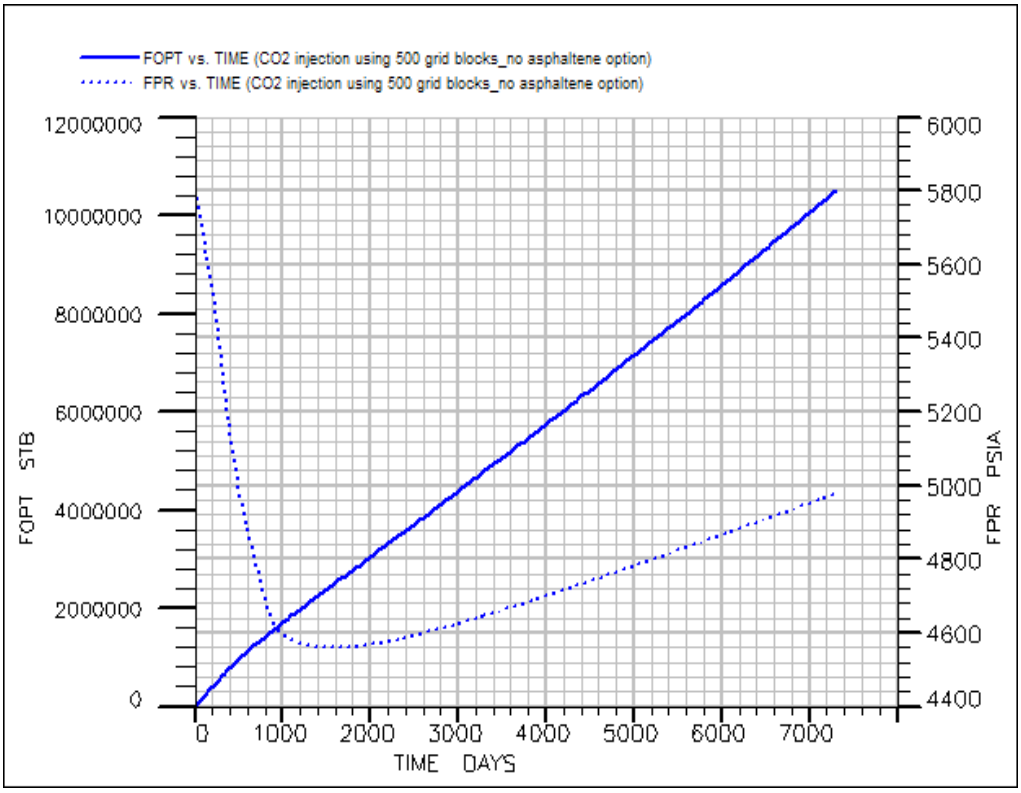

Figure 6. Cont.

b)

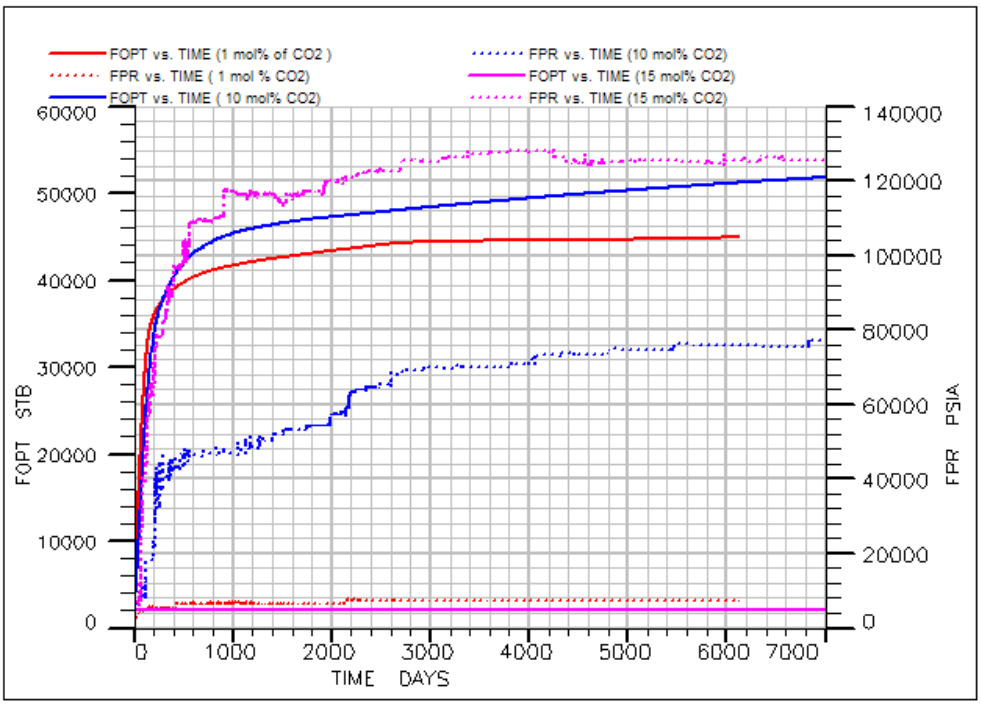

c)

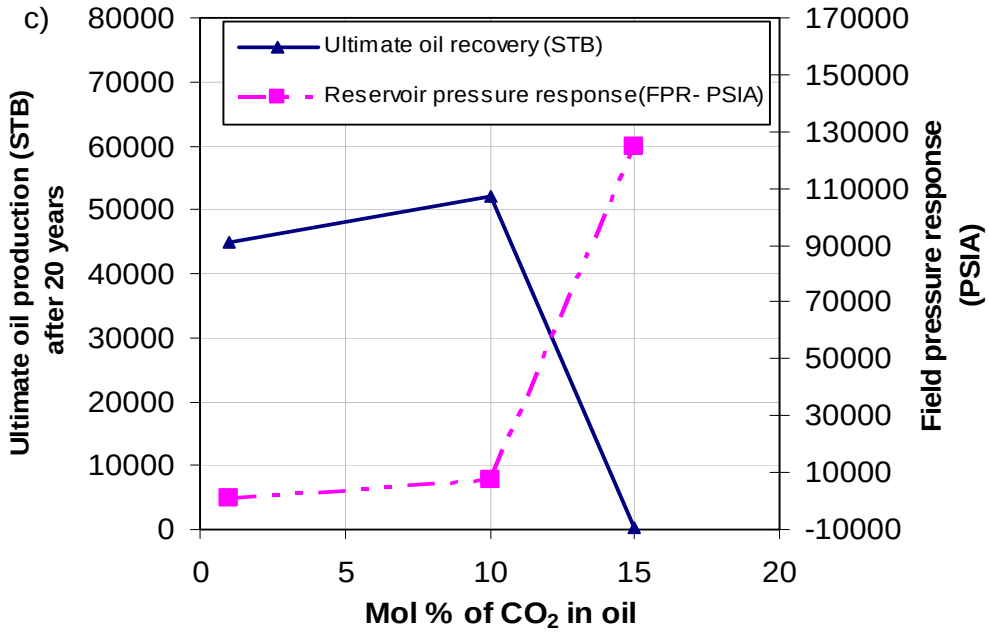

Figure 6. Cont.

d)

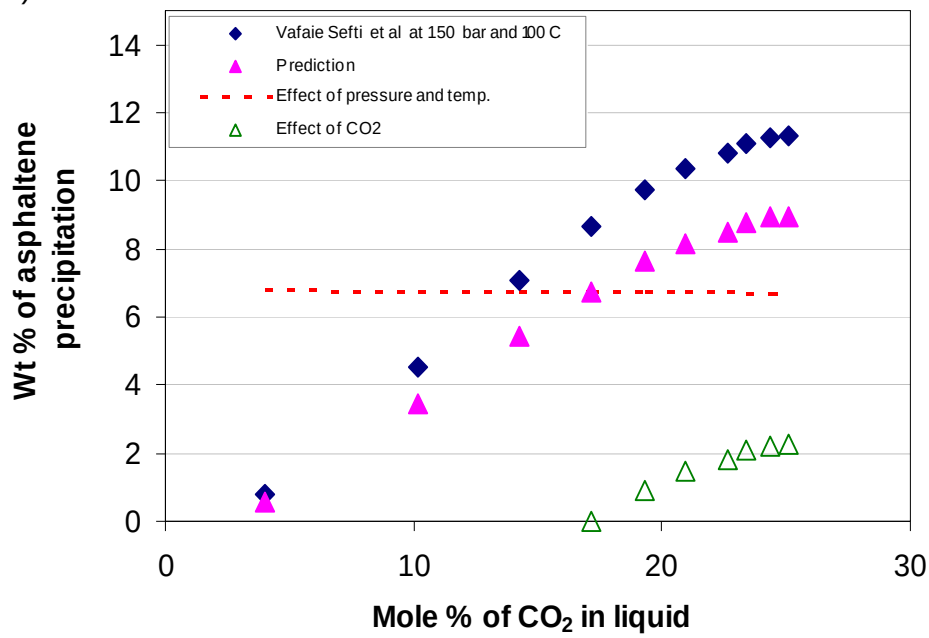

Figure 7. Comparison of oil recovery by water and miscible CO_2 flooding (well stream containing 100% CO_2) for 20 years simulation run. Tick and dotted lines represent oil recovery (STB) and the corresponding average field reservoir pressure (Psia), respectively).

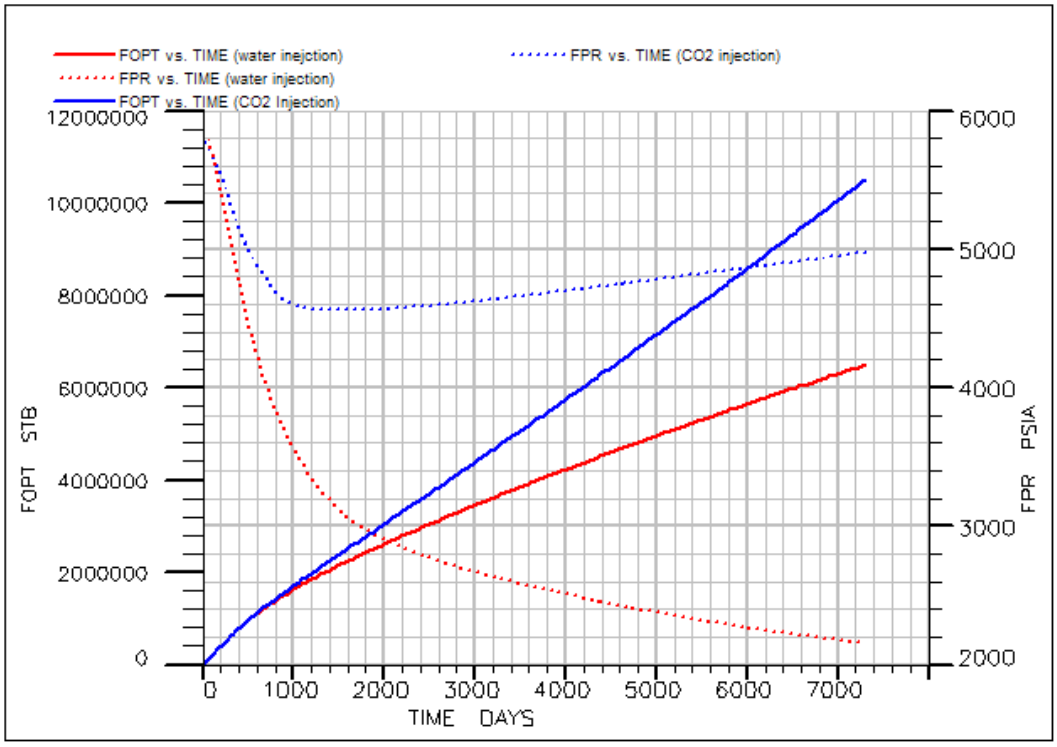

3. Experimental Section

3.1. Materials

3.1.1. Solid Phase

Outcrop chalk cores obtained from Stevns klint near Copenhagen Denmark of about 6–7cm in length, 3.8 cm in diameter, porosity of 44%–48% and absolute permeability of 3–5 mD are used. Table 2 is the core detailed description and its associated fluid content.

3.1.2. Fluids

The investigation is done on four types of oils: (a) *n*-decane (b) 0.005 M SA dissolved *n*-decane (reference), (c) model oil (0.35 wt % asphaltene dissolved in toluene, 0.005 M SA dissolved in *n*-decane (95% purity), and (d) crude oil (composition listed in Table 3). Distilled water and supercritical CO_2 are used as displacing fluids.

3.2. Oil model preparation procedure

Model oil system is prepared from asphaltene precipitated from crude oil in excess of *n*-heptane (1:40). The mixture is shaken for at least twice a day and left for 48 hours to equilibrate. It is then centrifuged and filtered through a 0.22 micrometer filter (Millipore), and dried for 1 day using a vacuum oven at room temperature. The dried asphaltenes (0.25 g) are then dissolved in toluene (19 g, i.e., 22 mL) and mixed with *n*-decane containing 0.005 M SA to obtain the model oil. The prepared model oil is filtered to remove the suspended materials.

Table 2. Core descriptions and fluid composition.

Core #	L(cm)	Wt-dry(g)	Porosity (%)	K (md)	Saturating fluid	S_{or} (%)	CO_2 mol injected (mol %)	Pressure and Temperature	Asphaltene content in feed oil (wt %)
1	6.90	115.77	46.4	4.9	n-C_{10}	18.38	93.53	90 bar/50 °C	
2	7.00	117.11	44.4	5.04	n-C_{10}	13.40	88.79	120 bar/ 70°C	
3	7.00	118.13	44.7	5.04	n-C_{10}	10.94	89.53	140 bar/ 80°C	
4	7.20	114.39	47.1	4.50	model oil	32.85	76.80	140 bar/ 80°C	0.35
5	7.20	118.29	44.8	4.19	model oil	21.04	85.2	120 bar/ 70°C	0.35
6	7.10	112.05	47.7	4.19	model oil	21.89	87.62	90 bar/50 °C	0.35
7	7.00	118.17	45.3	4.18	crude oil	64.44	85.12	140 bar/ 80 °C	10
8	7.00	117.37	44.7	4.18	crude oil	63.10	89.58	120 bar/ 70°C	10
9	7.00	115.74	45.9	4.18	crude oil	62.36	89.58	90 bar/50 °C	10

Table 3. Crude oil composition.

Components	Mol%
C_2	0.02
C_3	0.63
i-C_4	0.51
n-C_4	2.34
2,2-DM-C_3	0.01
i-C_5	2.32
n-C_5	3.51
C_6	6.28
C_7	6.7
C_8	6.7
C_9	5.77
C_{10+}	65.21 (287.38)*
Asphaltene	10 wt %
Density (50 °C)	0.87827 g/cm^3
Viscosity (50 °C)	0.0065 Pa·s

* Molecular weight of C_{10+}

3.3. Experimental procedure

3.3.1. CO_2 flooding

The procedure followed in CO_2 flooding has been extensively discussed in our previous work [40]. The major components of the experimental setup consist of a core holder, pressure regulator, two gas flow meters, pressure manometers, Gilson pump, three piston cells (two CO_2 piston cells and oil sample cell), graduated gas/oil separator and connected with PC controlled Labview (version 7.1) to monitor and continuously log the flooding data.

Oil saturated core samples are inserted into a horizontally placed core holder that consists of a steel cylindrical body and rubber/Teflon sleeve. A net overburden pressure of 20 bar is applied on the sleeve. Then, CO_2 injection is carried out in two modes, namely, immiscible and miscible flooding. Miscible and immiscible flooding, at pressures of 90 and 26 bar, respectively, are used for cores saturated with 0.005 M SA dissolved in *n*-C_{10} (used as reference oil + natural surfactant) at room temperature (25 °C). Miscible flooding is also done for *n*-decane, model oil and crude oil saturated cores at combined pressure and temperature of 90 bar/50 °C, 120 bar/70 °C and 140 bar/80 °C. CO_2 is injected from a piston cell via a flow meter (1) that records the in-flow properties of CO_2 (mass flow rate, density and total mass). A back pressure regulator is installed downstream the core to control the pressure during CO_2 flooding so that both gas and liquid effective permeabilities could be obtained to minimize CO_2 slip as recommended by Li *et al*. [43]. Prior to oil production, the back up pressure regulator is closed for about 5–10 minutes to equilibrate the system. The produced fluid from the core is collected in a graduated gas/oil separator where the fluid stream is separated to liquid and CO_2 gas. CO_2 gas is stored in a piston cell, not to be discharged into the atmosphere. The out-flow properties (mass flow rate, density and total mass) of the evolved gas are, also, recorded using flow meter (2)

connected to the separator. Minimium miscibility pressures (MMPs) used in this study are 90, 120 and 140 bar for temperatures of 50, 70 and 80 °C, respectively (for method of determination, see [40]).

3.3.2. Determination of asphaltene precipitation as a function of pressure

The measurement of asphaltene precipiatation as a function of pressure drop using core sample as a filter is schematically depicted in Figure 8. The unit consisted of a stainless steel Hassler-type core holder, Coriolis mass flow measuring system (Proline Promass 80), two pressure regulators, Gilson pump, Oven, two piston cells (one for confining pressure and the other for the oil model), ΔP Transducer (DELTA BAR-S PMD75), pressure gauges and Labview monitor 7.1.

Weighed chalk core sample initially dried at 130 °C is inserted into the core holder to simulate asphaltene deposition in the reservoir during pressure depletion. Confining pressure of approximately 20 bar over the injection pressure is maintained. Oil is charged into a piston cell and pressurized to the required working pressure of 100–130 bar in oven at isothermal temperature of 100 °C. The flowing rate of 0.5–3 mL/min is recorded and is dependent on the pressure drop (ΔP).

The inlet and outlet pressures of the core are controlled using backpressure regulators while the pressure drop across the sample is continuously monitored by a pressure transducer and displaced on the computer monitor. Constant pressure drop of 20, 50, 80 and 100 bars is maintained for each of the experiment. The oil injection continued until no oil production, the core is then dry at 130 °C, cooled down and weighted until a constant weight is obtained. The amount of asphaltene precipitated is determined by the weight difference between the final and initial dried weight.

Figure 8. Schematic of the setup used for flooding experiments.

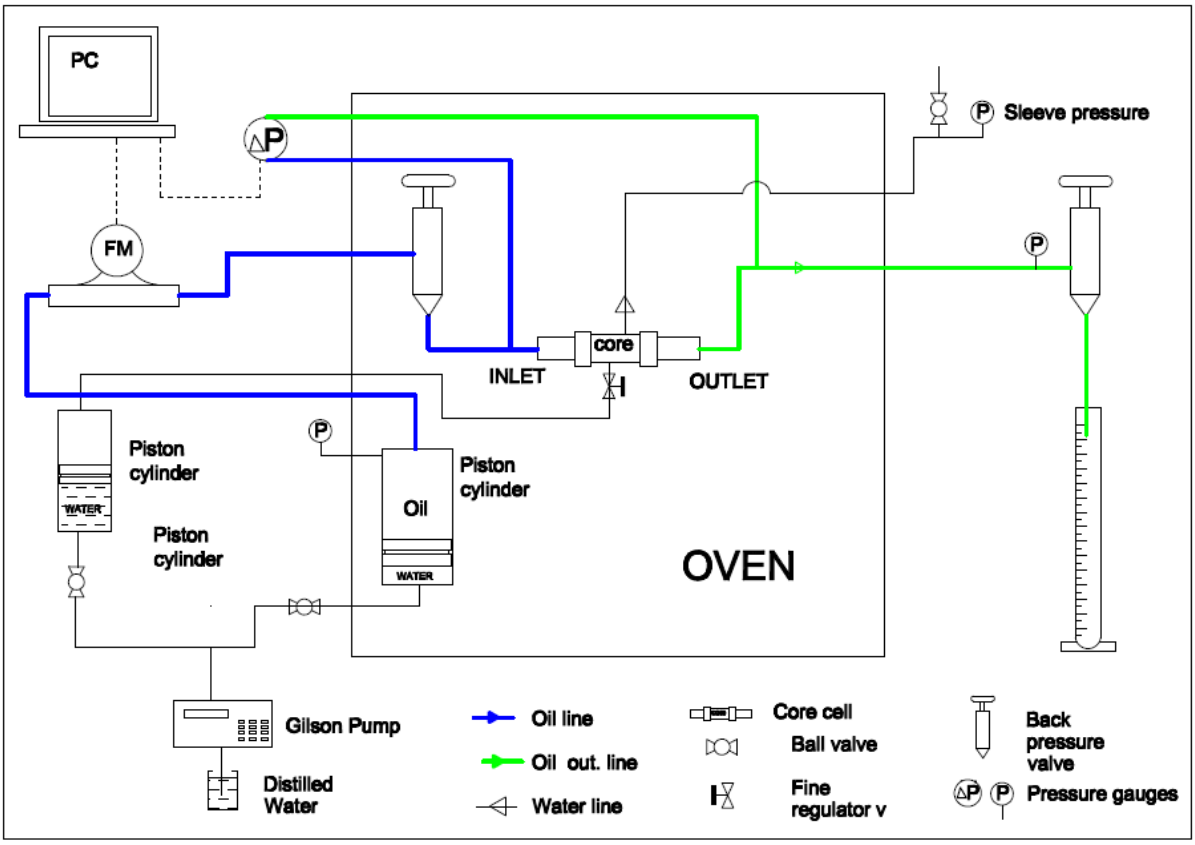

3.4. Simulation model

The simulation is done to investigate the effect of CO_2 on oil recovery on a large scale. A simple reservoir model grid of 50 × 1 × 10 (500 grid blocks) with dimensions of 7,500 × 600 × 150 ft is used, using a compositional simulator (Eclipse compositional model version 2008.1) with six components (C_1, CO_2, C_6, C_{10}, C_{15}, and C_{20}). Three phase model (water, oil and gas) and miscible option are selected for both asphaltenic and non-asphaltenic oils. For the asphaltenic oil, asphaltene precipitation option is selected. In the PVT section of the model, Peng-Robinson equation of state is specified for the calculation. Pseudo component is used for the properties of asphaltene, such as molecular weight of 1000 g/mol and density of 1.28 g/cm^3 to generate the fluid PVT properties at 50 °C and 90 bar. Experimental relative permeability data for *n*-decane and model oil saturated core at 90 bar and 50 °C are the relative permeability simulator input for non-asphaltenic and asphaltenic oils, respectively. The reservoir consists of total pore volume of 57.6 MM rb (Total fluid volume) and hydrocarbon pore volume (HCPV) of approximately 46.1 MM rb with average oil saturation of 0.8. The reservoir depth is taken to be 9,840 ft with two wells at the first grid block (injection well) and fifteth grid block (production well). Well bore diameter of 0.375 ft and wells control mode RESV (reservoir fluid volume rate) with upper limit of 2,000 rb/day is used. Bottom hole pressures of 8,890 and 200 psia are specified as injection and production pressure constraints, respectively. The simulation is run for 20 years. The oil composition and reservoir model inputs are listed in Table 4.

Table 4. Reservoir simulation input data and oil composition in mol %.

Parameter	Amount
Porosity	0.455-0.474
Absolute permeability (md)	3.2-5.0
Reservoir fluids	gas/oil/water
Oil density (lbs/ft^3) @ T=50ºC	48.44
Oil viscosity (cP) @ T=50ºC	5.5
Water density(lbs/ft^3)	62.43
Number of wells	2 (1 producer + 1 injector)
Depth of water oil contact (ft)	13120
Depth of gas oil contact (ft)	9825

Oil composition	Mol%
C_1	0.21
CO_2	1.94
C_6	3.04
C_{10}	5.9
C_{15}	8.73
C_{20}	80.18

4. Summary and Conclusions

EOR by miscible CO_2 flooding shows high ultimate oil recovery for non-asphaltenic oil compared with asphaltenic oil, as indicated by both the residual oil saturation at the cross points of the relative permeability curves. This may be explained based on fingering and oil trapping.

Asphaltene deposition is initiated by CO_2 when the critical content of CO_2 is exceeded. In other words if the injected CO_2 is maintained below the critical content point, higher oil recovery may be obtained from asphaltenic oil. The critical content point of CO_2 is dependent on oil composition, temperature and pressure and must be evaluated at early stage of screening methods for EOR. However, the combined temperature and pressure for miscible flooding must be taken into account, where it is shown that above 70 °C /120 bar, oil recovery declined.

Injection of CO_2 after at least 3 years of water injection as indicated by the simulation (for non-asphaltenic oil) is shown to have a significant effect on the incremental oil recovery. The cross point relative permeabilities as a function of CO_2 saturation are shown to decrease with asphaltene content. High residual oil saturation as asphaltene concentration increases, may suggest oil trapping.

A comparison between the oil recovery for asphaltenic oil by water and CO_2 flooding shows that above a certain temperature (70°C in this work) a reduction in oil recovery was observed by CO_2 flooding compared to water flooding. The reduction in oil recovery is attributed to increase of asphaltene precipitation with temperature. At pressure conditions higher than the bubble point pressure (bp) for the tested fluid, almost a linear relationship between pressure drop and the precipitated asphaltene (wt %) is obtained regardless of the injection pressure.

Acknowledgements

The authors would like to thank the University of Stavanger for the financial support of this project. We acknowledge Krzysztof piotr Dziadosz for his assistance in the experimental setup and Inger Johanne for her support and help in getting the chemicals needed.

References

1. Alavain, S.A.; Whitson, C.H. CO_2 IOR Potential in Naturally Fratured Haft Kel Field, Iran. Presented at the *International Petroleum Technology Conference*, Doha, Qatar, November 2005; IPTC 10641.
2. Moritis, G. Special Report: Enhanced Oil Recovery-2002 Worldwide EOR Survey. *Oil Gas J.* **2002**, *100*, 43-47.
3. Cuthiell, D.; Kissel, G.; Jackson, C.; Frauenfeld, T.; Fisher, D.; Rispler, K. Viscous Fingering Effects in Solvent Displacement of Heavy Oil. *J. Can. Pet. Technol.* **2006**, *45*, 29-39.
4. Agbalaka, C.; Dandekar, A.Y.; Patil, S.L.; Khataniar, S. The Effect of Wettability Alteration on Oil Recovery: A Review. Presented at *SPE Asia Pacific Oil & Gas Conference and Exhibition*, Perth, Australia, October 2008; SPE 114496.
5. Singh, M.; Mani, V.; Honarpour, M.M.; Mohanty, K.K. Comparison of Viscous and Gravity Dominated Gas-Oil Relative Permeabilities. *J. Pet. Sci. Eng.* **2001**, *30*, 67-81.

6. Li, D.; Lake, L.W. Scaling Fluid Flow through Heterogeneous Permeable Media. Presented at the *68th SPE Annual Technical Conference*, Houston, TX, USA, October 1993; SPE 26648.
7. Tang, G.-Q.; Leung, Y.; Castanier, L.M.; Sahni, A.; Gadelle, F.; Kumar, M.; Kovscek, A.R. An Investigation of the Effect of Oil Composition on Heavy Oil Solution Gas Drive. *SPE J.* **2006a**, *11*, 58-70.
8. Tang, G.-Q.; Sahni, A.; Gadelle, F.; Kumar, M.; Kovscek, A.R. Heavy-Oil Solution Gas Drive in Consolidated and Unconsolidated Rock. *SPE J.* **2006b**, *11*, 259-268.
9. Al-Wahaibi, Y.M.; Grattoni, C.A.; Muggeridge, A.H. Drainage and Imbibition Relative Permeabilities at Near Miscible Conditions. *J. Pet. Sci. Eng.* **2006**, *53*, 239-253.
10. Schembre, J.M.; Tang, G.Q.; Kovseck, A.R. Wettability Alteration and Oil Recovery by Water Imbibition at Elevated Temperatures. *J. Pet. Sci. Eng.* **2006**, *52*, 131-148.
11. Sedaee Sola, B.; Rashidi, F.; Babadagli, T. Temperature Effects on Heavy Oil/Water Relative Permeabilities of Carbonate Rocks. *J. Pet. Sci. Eng.* **2007**, *59*, 27-42.
12. Dana, E.; Skoczylas, F. Gas Relative Permeability and Pore Structure of Sandstones. *Int. J. Rock Mech. Min. Sci.* **1999**, *36*, 613-625.
13. Shalliker, R.A.; Guiochon, G. Understanding the Importance of the Viscosity Contrast between Sample Solvent Plug and the Mobile Phase and its Potential Consequence in Two-dimensional High-Performance Liquid Chromatography. *J. Chromatogr. A* **2009**, *1216*, 787-793.
14. Shalliker, R.A.; Catchpoole, H.J.; Dennis, G.R.; Guiochon, G. Visualizing Viscous Fingering in Chromatography Columns: High Viscosity Solute Plug. *J. Chromatogr. A* **2007**, *1142*, 48-55.
15. Rogers, J.D.; Grigg, R.B. A literature Analysis of the WAG Injectivity Abnormalities in the CO_2 Process. Presented at the *SPE/DOE Improved Oil Recovery Symposium*, Tulsa, OK, USA, April 2000; SPE 59329.
16. Akin, S.; Kovscek, A.R. Heavy-Oil Solution Gas drive: A Laboratory Study. *J. Pet. Sci. Eng.* **2002**, *35*, 33-48.
17. George, D.S.; Hayat, O.; Kovscek, A.R. A Microvisual Study of Solution Gas Drive Mechanisms in Viscous Oils. *J. Pet. Sci. Eng.* **2004**, *46*, 101-119.
18. Brailovsky, I.; Babchin, A.; Frankel, M.; Sivashinsky, G.A. Reduced Model for Fingering Instability in Miscible Displacement. *Phys. Lett. A* **2007**, *369*, 212-217.
19. Brailovsky, I.; Babchin, A.; Frankel, M.; Sivashinsky, G. Fingering Instability in Water-Oil Displacement. *Transp. Porous Media* **2006**, *63*, 363-380.
20. Musuuza, J.L.; Attinger, S.; Radu, F.A. An Extended Stability Criterion for Density Driven Flows in Homogeneous Porous Media. *Adv. Water Res.* **2009**, *32*, 796-808.
21. Mack, C. Colloid Chemistry of Asphalts. *J. Phys. Chem.* **1932**, *36*, 2901-2914.
22. Peng, L.; Yongan, G. Effects of Asphaltene Content on the Heavy Oil Viscosity at Different Temperatures. *Fuel* **2007**, *86*, 1069-1078.
23. Peng, J.; Tang, G.-Q.; Kovscek, A.R. Oil Chemistry and its Impact on Heavy Oil Solution Gas Drive. *J. Pet. Sci. Eng.* **2009**, *66*, 47-59.
24. Sohrabi, M.; Emadi, A.; Jamiolahmady, M.; Ireland, S.; Brown, C. Mechanisms of Extra-Heavy Oil Recovery by Gravity Oil Recovery Stable CO_2 Injection. Presented at the *International Symposium of the Society of Core Analysts*, Abu Dhabi, UEA, October-November, 2008; SCA 2008-20.

25. Baviere, M. *Basic Concepts in Enhanced Oil Recovery Processes*, Elsevier Applied Science: Essex, England, UK, 1991; p. 221.
26. Mullins, O.C. Review of the Molecular Structure and Aggregation of Asphaltenes and Petroleomics. *SPE J.* **2008**, *13*, 48-57**.**
27. de Boer, R.B.; Leerlooyer, K.; Eigner, M.R.P.; van Berge, A.R.D. Screening of Crude Oils for Asphalt Precipitation: Theory, Practice and the Selection of Inhibitors. *SPE Prod. Facil.* **1995**, *10*, 55-61.
28. Jamaluddin, A.K.M.; Creek, J.; Kabir, C.S.; McFadden, J.D.; D'Cruz, D.; Joseph, M.T.; Joshi, N.; Ross, B. A Comparison of Various Laboratory Techniques to Measure Thermodynamic Asphaltene Instability. Presented at the *SPE Asia Pacific Improved Oil Recovery Conference*, Kuala Lumpur, Malaysia, October 2001; SPE 72154.
29. Islam, M.R. Role of Asphaltenes on Oil Recovery and Mathematical Modeling of Asphaltene Properties. In *Asphaltenes and Asphalts, I. Developments in Petroleum Science*, Yen, T.F., Schilingarian, G.V., Eds.; Elsevier: Amsterdam, The Netherlands, 1994; Vol. 40, pp. 249-298.
30. Leontaritis, K.J.; Mansoori, G.A. Asphaltene Deposition: A Survey of Field Experiences and Research Approaches. *J. Pet. Sci. Eng.* **1988**, *1*, 229-239.
31. Danesh, A.; Krinis, D; Henderson, G.D.; Peden, J.M. Pore Level Visual Investigation of Miscible and Immiscible Displacement. *J. Pet. Sci. Eng.* **1989**, *2*, 167-177.
32. Newberry, M.E.; Barker, K.M. Organic Formation Damage Control and Remediation. Presented at the *SPE International Symposium on Formation Damage Control*, Lafayette, LA, USA, February 2000; SPE 58723.
33. Hu, Y.-F.; Li, S.; Liu, N.; Chu, Y.-P.; Park, S.J.; Mansoori, G.A.; Guo, T.-M. Measurement and Corresponding States Modelling of Asphaltene Precipitation in Jilin Reservoir Oils. *J. Pet. Sci. Eng.* **2004**, *41*, 199-212.
34. Pooladi-Darvish, M.; Firoozabadi, A. Solution-Gas Drive in Heavy Oil Reservoirs. *J. Can. Pet. Technol.* **1999**, *38*, 54-61.
35. Gielen, D.; Unander, F. Alternative Fuels: An Energy Technology Perspective. Presented at the *International Energy Agency (IEA) Workshop on Technology Issues for the Oil and Gas Sector*, Paris, France, January 2005; ETO/2005/01.
36. Speight, J.G. *Petroleum Analysis and Evaluation, Petroleum Chemistry and Refining*. Taylor & Francis: Washington, DC, USA, 1999.
37. Branco, V.A.M.; Mansoori, G.A.; De Almeida Xavier, L.C.; Park, S.J.; Manafi, H. Asphlatene Focculation and Collapse from Petroleum Fluids. *J. Pet. Sci. Eng.* **2001**, *32*, 217-230.
38. Burke, N.E.; Hobbs, R.E.; Kashon, S.F. Measurement and Modeling of Asphaltene Precipitation. *J. Pet. Technol.* **1990**, *42*, 1440-1446.
39. Werner, A.; Behar, F.; de Hemptinne, J.C; Behar, E. Viscosity and Phase Behaviour of Petroleum Fluids with High Asphaltene Contents. *Fluid Phase Equilib.* **1998**, *147*, 343-356.
40. Hamouda, A.A.; Chukwudeme, E.A.; Mirza, D. Investigating the Effect of CO_2 Flooding on Asphaltenic Oil Recovery and Reservoir Wettability. *Energy Fuels* **2009**, *23*, 1118-1127.
41. Lindeberg, E.; Torleif, H. EOR by Miscible CO_2 Injection in the North Sea. Presented at the *SPE/DOE Ninth Symposium on Improved Oil Recovery*, Tulsa, OK, USA, April 1994; SPE/DOE 27767.

42. Hirschberg, A.; DeJong, L.N.J.; Schipper, B.A.; Meijer, J.G. Influence of Temperature and Pressure on Asphaltene Flocculation. *SPE J.* **1984**, *24*, 283-293.
43. Li, S.; Dong, M.; Li, Z. Measurement and Revised Interpretation of Gas Flow Behavior in Tight Reservoir Cores. *J. Pet. Sci. Eng.* **2009**, *65*, 81-88.